Climate
of the Past

Iron fluxes to Talos Dome, Antarctica, over the past 200 kyr

P. Vallelonga[1,2]**, C. Barbante**[2,3,4]**, G. Cozzi**[2]**, J. Gabrieli**[2]**, S. Schüpbach**[3,5]**, A. Spolaor**[3]**, and C. Turetta**[2]

[1]Centre for Ice and Climate, Niels Bohr Institute, University of Copenhagen, Juliane Maries Vej 30,
2100 Copenhagen, Denmark
[2]Institute for the Dynamics of Environmental Processes (IDPA) – CNR, University of Venice, Dorsoduro 2137,
30123 Venice, Italy
[3]Department of Environmental Sciences, Informatics and Statistics, University Ca' Foscari of Venice, Dorsoduro 2137,
30123 Venice, Italy
[4]Accademia Nazionale dei Lincei, Centro B. Segre, via della Lungara 10, 00165, Rome, Italy
[5]Physics Institute, Climate and Environmental Physics, University of Bern, Sidlerstrasse 5, 3012, Bern, Switzerland

Correspondence to: P. Vallelonga (ptravis@nbi.ku.dk)

Abstract. Atmospheric fluxes of iron (Fe) over the past 200 kyr are reported for the coastal Antarctic Talos Dome ice core, based on acid leachable Fe concentrations. Fluxes of Fe to Talos Dome were consistently greater than those at Dome C, with the greatest difference observed during interglacial climates. We observe different Fe flux trends at Dome C and Talos Dome during the deglaciation and early Holocene, attributed to a combination of deglacial activation of dust sources local to Talos Dome and the reorganisation of atmospheric transport pathways with the retreat of the Ross Sea ice shelf. This supports similar findings based on dust particle sizes and fluxes and Rare Earth Element fluxes. We show that Ca and Fe should not be used as quantitative proxies for mineral dust, as they all demonstrate different deglacial trends at Talos Dome and Dome C. Considering that a 20 ppmv decrease in atmospheric CO_2 at the coldest part of the last glacial maximum occurs contemporaneously with the period of greatest Fe and dust flux to Antarctica, we confirm that the maximum contribution of aeolian dust deposition to Southern Ocean sequestration of atmospheric CO_2 is approximately 20 ppmv.

1 Introduction

Polar ice cores allow detailed reconstructions of atmospheric composition and aerosol loading which are important for understanding the origins of climate transitions as well as

potential feedback effects (Wolff et al., 2006; Fischer et al., 2010). Mineral aerosol (dust) plays a role in several direct and indirect climate feedback processes (Maher et al., 2010) with extremely large (up to 40-fold) changes in dust fluxes at polar and high-latitude regions between glacial and interglacial climates (Fischer et al., 2007). In central Antarctica, increased dust fluxes arise due to enhancement of the arid dust-deflation zones of southern South America in combination with reduced washout of dust (Lambert et al., 2008). Isotopic (Delmonte et al., 2010; Vallelonga et al., 2010) and modelling (Li et al., 2008; Mahowald et al., 2005) investigations indicate changes in dust provenance from glacial to interglacial climates, with a dominant southern South American dust source during the glacial maxima and enhanced dust entrainment from Australia and local Antarctic ice-free areas during interglacial periods. Marine sediments demonstrate an increased production and/or transport of dust from southern South American sources during the late Pleistocene (Martinez-Garcia et al., 2009).

Records of past atmospheric fluxes of dust and elements such as iron (Fe) are essential for testing the "Iron hypothesis" proposed by Martin (1990), in which CO_2 drawdown in some oceanic zones is controlled not by the availability of macronutrients, such as nitrogen and phosphorus, but by the availability of micronutrients essential for biological growth, particularly Fe. Trials of ocean surface Fe addition in High-Nutrient Low-Chlorophyll (HNLC) zones of the southern and equatorial Pacific Oceans have reinforced the possibility

that past changes in iron deposition could have been significant for CO_2 drawdown (Sigman et al., 2010; Smetacek et al., 2012). A complementary mechanism for the transport of nutrients to HNLC zones is wind-driven upwelling of nutrient-rich deep waters: Anderson et al. (2009) identified changes in opal fluxes from a southern ocean sediment core which may have been due to shifts in the latitude of southern westerlies during the last termination (T_1). Such shifts consequently alter southern ocean circulation, the strength of abyssal upwelling and nutrient transport to the subantarctic oceanic zone. Syntheses of terrestrial, marine and ice core dust data are essential for the contribution of aeolian dust deposition to Fe fertilisation to be accurately evaluated (Maher et al., 2010).

Records of aeolian Fe inputs to Antarctica are available for two sites: EPICA Dome C (EDC) (Gaspari et al., 2006; Wolff et al., 2006) on the central Eastern plateau and coastal Law Dome (Edwards et al., 2006), showing marked differences in glacial-interglacial Fe fluxes and ratios. EDC samples were leached at pH 1 for > 24 h (identical to this study) while the Law Dome samples were acidified for 1 month, thus, allowing for more complete dissolution of acid-labile Fe. An early evaluation of oceanic dust fertilisation employed non-sea salt Ca^{2+} ($nssCa^{2+}$) as a proxy for Fe (Röthlisberger et al., 2004). Consequently, the biological pump has been calculated to account for 10 to 50 % of the 80–100 ppmv CO_2 changes observed over glacial-interglacial transitions (Martinez-Garcia et al., 2009; Fischer et al., 2010). Here, we present a record of Fe fluxes at Talos Dome (TD) for the past 200 kyr to assess atmospheric dust deposition controls on Southern Ocean paleoproductivity.

2 Experimental

Samples were obtained from the TALDICE ice core (159°11′ E, 72°49′ S; altitude 2315 m a.s.l.; annual mean temperature −41 °C; snow accumulation 80 mm water equivalent yr^{-1}; (Stenni et al., 2011); further information is available from www.taldice.org). The TALDICE-1a chronology (Buiron et al., 2011; Schüpbach et al., 2011) has an uncertainty of 300 yr over T_1 and less than 600 yr over MIS 3. Discrete samples were obtained from a 32 mm × 32 mm section of the inner part of the ice core following Continuous Flow Analysis (Kaufmann et al., 2008). Ice was melted on a gold-coated brass melthead at a rate of 3 cm min^{-1}, with discrete samples collected in coulter counter accuvettes at a rate of 0.5 mL min^{-1}. Each 15 mL sample integrated a metre of melted ice. Samples were transported frozen to Italy for analysis.

The sample preparation and analytical methods have been reported previously (Barbante et al., 1999). Samples were prepared in a shipping container converted into a particle-free laboratory, with HEPA-filtered overpressured working spaces rated to Class 10 to 100 (US Fed. Std 209E, equivalent to ISO 4 to 5). Melted samples were acidified to pH 1 using sub-boiling distilled HNO_3 (Romil, Cambridge, UK) and analysed at least 24 h later by Inductively Coupled Plasma Sector Field Mass Spectrometry (ICP-SFMS; FinniganTM ELEMENT2, Thermo Fisher Scientific Inc., Bremen, Germany) coupled to an APEX Q desolvating introduction unit (Elemental Scientific, Omaha, NE, USA). The detection limit, defined as three times the standard deviation of the instrument blank, was 0.029 ng g^{-1}, with precisions of 16 % for Holocene samples and 10 % for Last Glacial Maximum (LGM) samples. We report here acid leachable Fe concentrations, following the techniques described by Gaspari et al. (2006), in order to compare Talos Dome Fe fluxes directly to those reported for EPICA Dome C. We acknowledge that the Fe fluxes reported here under-represent total Fe in the samples by approximately 35 % (LGM) to 70 % (Holocene) (Gaspari et al., 2006). Despite this, we observe that LGM/Holocene Fe ratios for Talos Dome are similar to those found for dust (Table 1) and, hence, should not affect the conclusions drawn here. It has been demonstrated that at least one month of acidification is required to completely dissolve Fe-bearing aerosol particles in ice (Edwards et al., 2006). Fluxes were calculated by multiplying Fe concentrations by TALDICE-1a accumulation rates (uncertainty ±20 %). The time period integrated by each sample varies from about 15 yr at 0.6 kyr before the present (BP, 1950 CE) to 30 yr at 15 kyr BP and 700 yr by MIS 6 (150 kyr BP). TALDICE $nssCa^{2+}$ concentrations have been calculated from Ca^{2+} and Na^+ CFA data (1 m averages) using the sea salt and average crustal Ca^{2+}/Na^+ ratios described in Bigler et al. (2006), while the EDC $nssCa^{2+}$ fluxes are from Röthlisberger et al. (2002). To highlight the trends shown in the figures, we show running average smoothing filters overlaying the data.

3 Results and discussion

TALDICE Fe fluxes are shown in Fig. 1, demonstrating a well-described pattern of higher dust and Fe concentrations during colder climate periods, and lower dust and Fe fluxes during warmer climate periods (Wolff et al., 2006). For consistency, we only compare Talos Dome (Delmonte et al., 2010) and EDC (Lambert et al., 2008) dust data determined by coulter counter instruments. Despite the variable sampling frequency, glacial dust fluxes are similar at TD and EDC, with more dust deposited during MIS 2 with respect to MIS 6. In contrast, similar Fe fluxes are observed for TD and EDC during MIS 6, but TD fluxes are greater than those at EDC during MIS 2. Greater Fe fluxes and variability were observed at TD compared to EDC during the Holocene. In Table 1, TD Fe concentrations and fluxes are compared with other Antarctic sites for which Fe fluxes are available. These show that Holocene fluxes of Fe at the coastal sites of Talos Dome and Law Dome are an order of magnitude higher

Table 1. Deposition of Antarctic Fe and dust before and after the last deglaciation. Talos Dome Fe data compared to EPICA Dome C (EDC) (Gaspari et al., 2006; Delmonte et al., 2010) and Law Dome (Edwards et al., 2006). Dust concentrations and fluxes are also shown for EDC and Talos Dome (Delmonte et al., 2010). Note that Fe and dust concentrations are shown in normal font while fluxes are shown in bold font. Coefficients of variability (CV) have been calculated for Talos Dome and EDC Fe fluxes. Indicative Holocene accumulation rates are also shown for comparative purposes.

	Talos Dome		Law Dome	Dome C	
Holocene accumulation ($m\,H_2O$ eq. yr^{-1})	0.08		0.8	0.034	
Concentrations ($ng\,g^{-1}$) **Fluxes ($10^{-2}\,mg\,m^{-2}\,yr^{-1}$)**	Fe	Dust	Fe	Fe	Dust
Holocene (2–16.5 kyr BP)	1.5 **9** **(CV 0.6)**	20 **130**	0.06 **4.5**	0.2 **0.7** **(CV 0.4)**	15 **40**
LGM (18–25 kyr BP)	14.8 **45** **(CV 0.3)**	250 **850**	6.4 **45**	16 **24** **(CV 0.3)**	750 **1000**
LGM/Holocene	10 **5**	12 **6**	107 **10**	74 **36**	50 **25**

than at Dome C, although LGM fluxes are of the same order of magnitude. For Talos Dome, the elevated interglacial dust flux has been attributed to the deglacial activation of proximal dust deflation zones in Victoria Land, Antarctica (Albani et al., 2012), which contribute dust to coastal areas, but not to the central Antarctic plateau (Delmonte et al., 2013). For Law Dome, dust fluxes or particle size distributions have not been reported, so the source(s) of interglacial dust cannot be speculated upon. The deposition of dust from local (Antarctic) sources at Law Dome cannot be discounted, as locally-sourced dust has also been observed at Berkner Island, based on the analysis of Sr and Nd isotopic compositions in recent snowpack (Bory et al., 2010).

Deglacial variability of Fe, dust and non-sea salt (nss) Ca^{2+} fluxes are shown in Fig. 2, showing a clear decoupling of coastal Antarctica (TD) from central Antarctica (EDC) from 20 to 10 kyr BP. As mentioned previously, fluxes of these parameters were similar during the LGM, but have been consistently greater at TD since the deglaciation. This deglacial decoupling trend was first observed by Delmonte et al. (2010) for TD dust fluxes and particle size distributions and was attributed to the activation of local (Victoria Land) dust deflation areas during the deglaciation. Albani et al. (2012) reported TD dust particle size distributions at greater temporal resolution (fine/coarse particle size ratios are also shown in Fig. 2), finding a similar deglacial decoupling, which was then followed by a convergence of TD and EDC dust fluxes since 8 kyr BP (Fig. 3), as a result of changes to atmospheric transport patterns around the Ross Sea embayment. The retreat of the Ross ice shelf grounding line appears to have led to a preference for the transport of air

masses over the Ross Sea, which is not conducive to the deflation of dust in high-altitude areas of Victoria Land.

Dust fluxes to Talos Dome and EDC diverge during the last deglaciation, a period of large-scale atmospheric reorganisation across Antarctica and the sub-Antarctic region. Post-glacial changes in atmospheric transport and/or provenance have been observed for dust particle sizes (Delmonte et al., 2004) and dust components such as Rare Earth Elements (Wegner et al., 2012; Gabrielli et al., 2010) and Pb isotopes (Vallelonga et al., 2010). The Talos Dome dust record does not demonstrate the "pre-Holocene dust minimum" observed in EDC, DB and Komosmolskaia ice cores in central East Antarctica (Delmonte et al., 2004), suggesting that different atmospheric transport regimes develop in these different sectors of Antarctica as interglacial conditions develop. Atmosphere-ocean coupled models, supported by stable water isotope data, indicate that the various sectors of Antarctica have differing responses to rapid climate variations such as the deglacial (Buiron et al., 2012). Further, systematic variations have been observed for Rare Earth Element compositions in EDC ice which have been attributed to changing dust provenance during and after the deglaciation (Gabrielli et al., 2010).

Such variability can also be observed in the deglacial Fe flux record (Fig. 2), as a distinctive Fe peak in the Antarctic Cold Reversal (ACR) observed at EDC (Gaspari et al., 2006) between 13.0 and 12.7 kyr BP is not present at TD. A similar-size Fe peak is observed later at TD from 12.1 to 11.8 kyr BP. The core chronologies in this period have been synchronized by CH_4 tiepoints, so there is no possibility of attributing this to a misalignment or a dating error. Instead, it appears that these Fe peaks reflect different dust histories
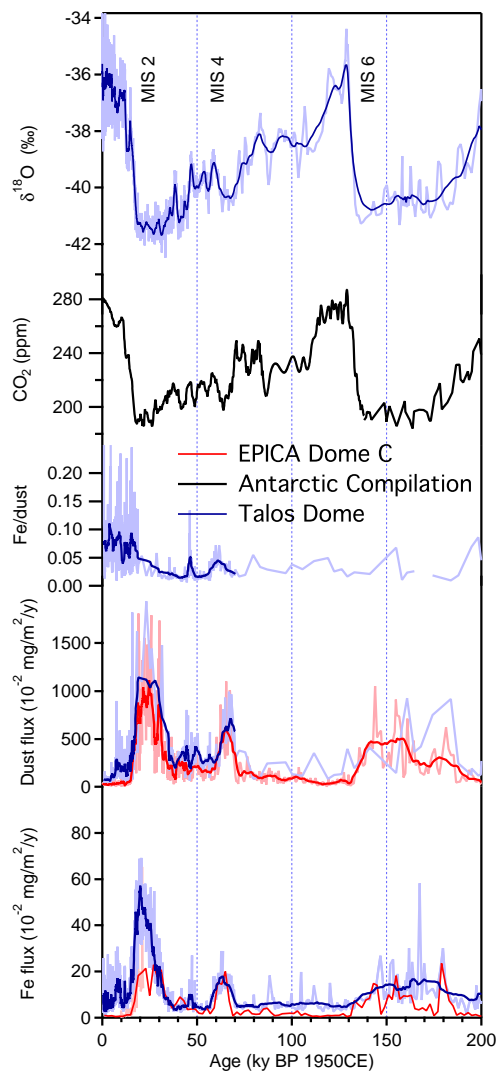
Fig. 1. Talos Dome Fe (this work) and dust (Delmonte et al., 2010) fluxes and $\delta^{18}O$ (Stenni et al., 2011) compared to Fe (Wolff et al., 2006) and dust (Lambert et al., 2008) fluxes at EPICA Dome C. All dust concentrations were determined by coulter counter. CO_2 concentrations were compiled from various Antarctic ice cores for the period 0.2–138 kyr BP (Schilt et al., 2010) and from EDC before 138 kyr BP (Lüthi et al., 2008). Thick lines show various box smoothing filters that have been applied to EDC dust fluxes (11 pt, 0–200 kyr BP) and Talos Dome $\delta^{18}O$ data (15 pt, 0–200 kyr BP), Fe/dust ratios (19 pt, 0–70 kyr BP), dust fluxes (11 pt, 0–70 kyr BP) and Fe fluxes (19 pt, 0–80 kyr BP; 9 pt, 80–200 kyr BP).

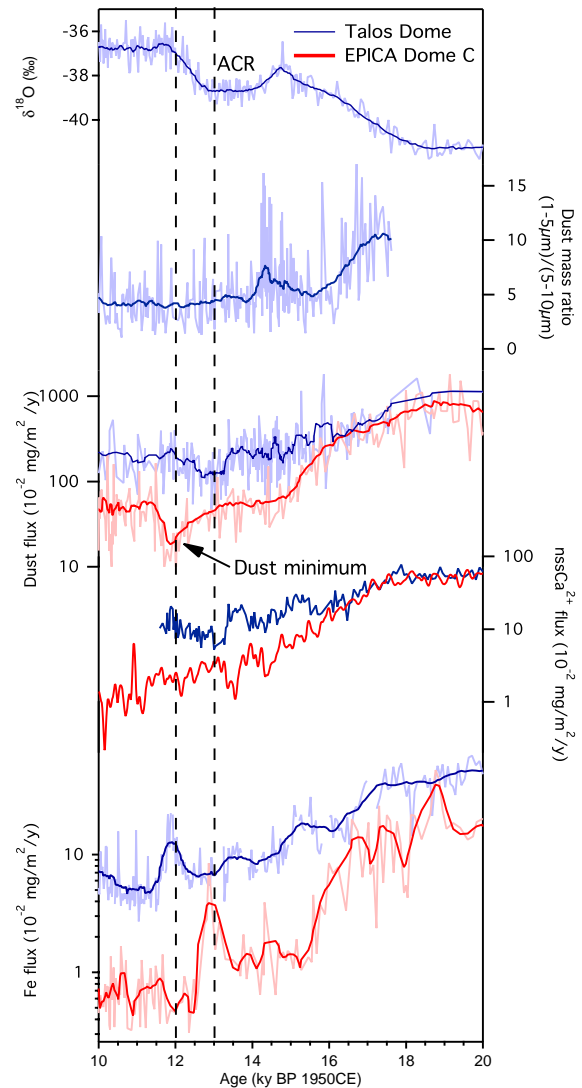**Fig. 2.** Deglacial changes in Fe, nssCa^{2+} and dust at Dome C and Talos Dome. TALDICE $\delta^{18}O$ values are from (Stenni et al., 2011). Fine (1–5 μm)/coarse (5–10 μm) dust particle ratios are from Albani et al. (2012) and dust fluxes are from Delmonte et al. (2010). All dust concentrations were determined by coulter counter. EPICA Dome C dust fluxes are from Lambert et al. (2008). nssCa^{2+} data are shown for TD (this study) and EDC (Röthlisberger et al., 2002) ice cores. Deglacial EDC Fe fluxes are from Gaspari et al. (2006). The vertical dashed lines, located at 11.9 and 12.9 kyr BP, highlight enhanced Fe fluxes which occur independently of dust fluxes at Talos Dome and Dome C, respectively.

for different sectors of Antarctica over the deglacial. Figure 1 shows greater TD Fe/dust ratios during the Holocene compared to the glacial, suggestive of a change in TD dust sources from the LGM to the Holocene.

The high resolution of the TALDICE record also allows millennial-scale variations to be evaluated over the Holocene, as shown in Fig. 3. Iron fluxes varied between higher ($> 10^{-1}$ mg m^{-2} a^{-1}) and lower

($< 5 \times 10^{-2}$ mg m^{-2} a^{-1}) values throughout the Holocene, with highest values during the mid-Holocene (7–10 kyr BP). The period of higher Fe fluxes from 7–10 kyr BP was not matched by consistent changes in dust flux, $\delta^{18}O$ or Fe/dust ratio although there was some tendency toward a greater proportion of fine dust particles at Talos Dome between 7 and 10 kyr BP (Albani et al., 2012). In contrast, there was
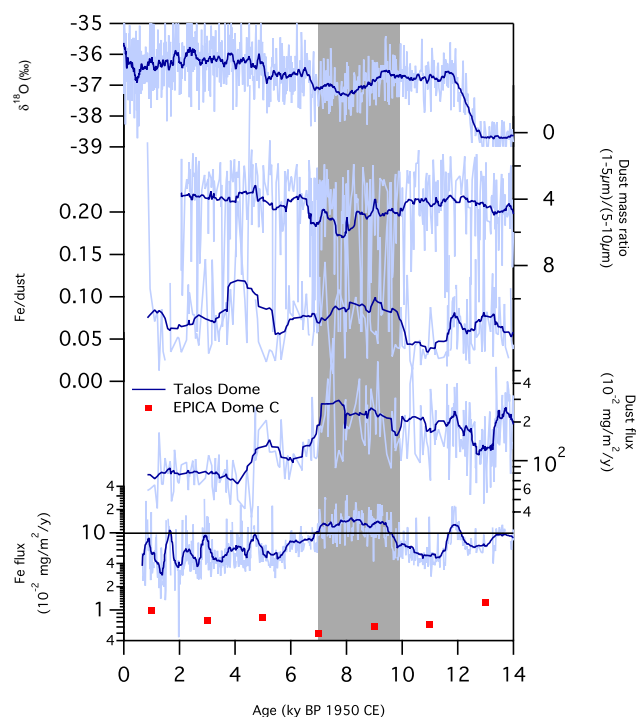
Fig. 3. Holocene Fe (this work) and dust (Delmonte et al., 2010) fluxes and fine (1–5 µm)/coarse (5–10 µm) dust particle ratios (Albani et al., 2012) in the TALDICE ice core (blue lines). TALDICE δ^{18}O values are from (Stenni et al., 2011). EPICA Dome C dust fluxes (Wolff et al., 2006) are also shown (red squares). Note the fine/coarse dust particle ratios are plotted here on a reversed scale. The horizontal black line delineates the period of enhanced Fe fluxes from 7 to 10 kyr BP.

Fig. 4. Comparison of LGM Fe fluxes and late glacial drawdown of CO_2. TALDICE δ^{18}O paleotemperature values are from (Stenni et al., 2011). CO_2 concentrations were compiled from various Antarctic ice cores (Lüthi et al., 2008; Schilt et al., 2010) while Fe fluxes are shown for TD (this work) and EDC (Wolff et al., 2006; Gaspari et al., 2006) ice cores.

a consistent change in dust and Fe fluxes and dust size fractions after 7 kyr BP (Fig. 3). This is consistent with a steady increase in δ^{18}O, coinciding with the retreat of the Ross ice shelf and resulting in shifts in regional atmospheric transport patterns away from dust deflation trajectories (Albani et al., 2012). After 7 kyr BP, there are clear decreases in Fe and dust fluxes to Talos Dome, as well as tendency toward deposition of coarser dust. The TD Holocene Fe record displays many spikes with up to 6-fold flux variations in adjacent samples, attributed to the influence of large dust particles emitted from local sources. Delmonte et al. (2010) observed that 5–20 µm diameter dust particles account for 60 to 70 % of total dust mass during the Holocene. By comparison, large particles constitute less than 20 % of total TD dust mass during MIS 2.

Figure 2 also shows clearly that deglacial trends of nssCa^{2+}, dust and Fe have many individual features on millennial to centennial timescales, which inhibit their applicability as proxies for each other. It is recognised that the common terrestrial sources of dust, Fe and nssCa^{2+} enable these parameters to be used to represent each other on glacial-interglacial time scales, but such commonality cannot be assumed for shorter time periods (Wolff et al., 2006).
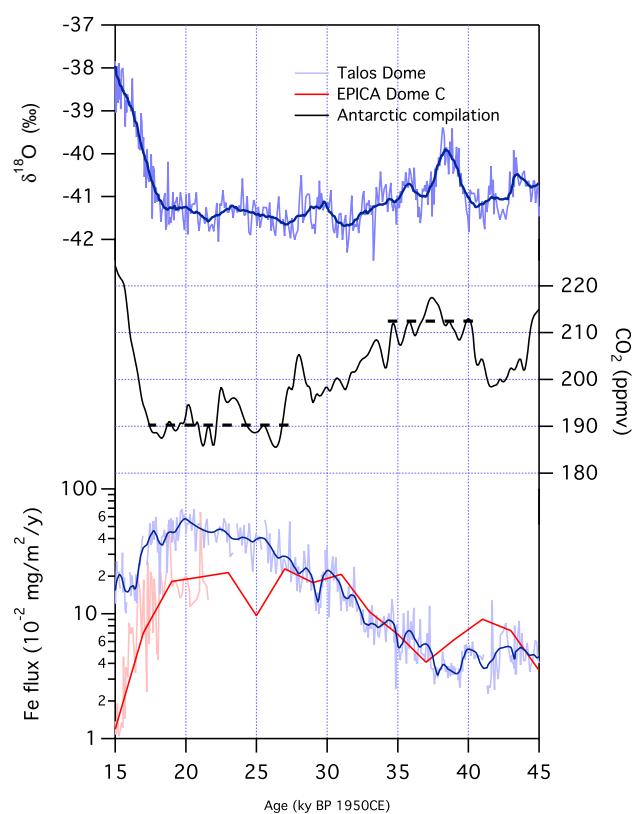
Comparing the EDC dust trend to Fe and nssCa^{2+} at EDC, we see that the dust minimum at 11.9 kyr BP is not mirrored by minima in Fe or nssCa^{2+}. Similarly, deglacial peaks in Fe at EDC (12.9 kyr BP) and Talos Dome (11.9 kyr BP) occur in the absence of corresponding features in deglacial dust fluxes. Some additional noise may be induced in the nssCa^{2+} record because they rely on Na$^+$ fluxes to calculate the contribution of Ca from marine salts. Nonetheless, the variability observed in Fe, an element derived solely from crustal sources, compared to dust is enough to demonstrate that neither dust nor nssCa^{2+} should be used to estimate Fe fluxes on millenial or centennial time scales.

In the absence of Fe data, Röthlisberger et al. (2004) evaluated the response of the biological pump to varying dust fluxes by considering changes in EDC nssCa^{2+} over the period 60–30 kyr BP. They observed large nssCa^{2+} variations and small CO_2 variations, concluding that Fe fertilisation could account for at most 20 ppmv of CO_2 drawdown. We apply a similar approach for the LGM, taking advantage of the Fe flux records now available for EDC and TD (Fig. 4). We note that the atmospheric concentration of CO_2

decreases from 212 ppmv (35–40 kyr BP) to 190.6 ppmv (17–27 kyr BP) at the same time as dust and Fe fluxes increase to their LGM peak. Aeolian contributions to marine primary productivity before 37 kyr BP can be considered minimal. On this basis, we find a comparable result to those of Röthlisberger et al. (2004), that approximately 20 ppmv of the glacial-interglacial atmospheric CO_2 change can be attributed to atmospheric transport of mineral dust to the Southern Ocean. We acknowledge that the Fe data reported here are based on samples acidified to pH 1 and, although they do not allow calculation of the Fe dissolved in the oceans during the LGM, they are still valid for evaluating the relative change in Fe deposited to the Southern Ocean from 35–40 kyr BP to 17–27 kyr BP.

4 Conclusions

We show that deglacial Fe, dust and $nssCa^{2+}$ fluxes varied across Antarctica, with TALDICE Fe fluxes consistently greater than those of EDC due to the deglacial activation of Antarctic coastal dust deflation sites as well as changing atmospheric transport patterns across Antarctica. Further, we show that fluxes of dust, $nssCa^{2+}$ and Fe can vary considerably from each other on millennial to centennial time scales. Based on the similar timing of LGM CO_2 drawdown and heightened Fe fluxes, we follow the technique of Röthlisberger et al. (2004) to attribute a maximum contribution of 20 ppmv of glacial-interglacial CO_2 variability to aeolian dust deposition over the Southern Ocean. Iron fluxes during MIS 6 were substantially less than those of MIS 2, implying that Fe fertilisation contributed less to the similar-magnitude CO_2 increase during the penultimate deglaciation. One of the assumptions of Röthlisberger et al. (2004) was that of constant Fe solubility in dust. Ongoing studies should consider the solubility of Fe deposited to the sub-Antarctic regions: Fe/dust ratios calculated from Table 1 vary from 0.01 to 0.02 (EDC) and from 0.05 to 0.08 (TD), potentially reflecting different dust sources, transport pathways and atmospheric residence times, as well as different chemical properties such as Fe speciation (Spolaor et al., 2012, 2013) or colloid formation.

Edited by: E. Isaksson

References

Albani, S., Delmonte, B., Maggi, V., Baroni, C., Petit, J.-R., Stenni, B., Mazzola, C., and Frezzotti, M.: Interpreting last glacial to Holocene dust changes at Talos Dome (East Antarctica): implications for atmospheric variations from regional to hemispheric scales, Clim. Past, 8, 741–750, doi:10.5194/cp-8-741-2012, 2012.

Anderson, R. F., Ali, S., Bradtmiller, L. I., Nielsen, S. H. H., Fleisher, M. Q., Anderson, B. E., and Burckle, L. H.: Wind-Driven Upwelling in the Southern Ocean and the Deglacial Rise in Atmospheric CO_2, Science, 323, 1443–1448, doi:10.1126/science.1167441, 2009.

Barbante, C., Cozzi, G., Capodaglio, G., Van de Velde, K., Ferrari, C. P., Boutron, C. F., and Cescon, P.: Trace element determination in alpine snow and ice by double focusing inductively coupled plasma mass spectrometry with microconcentric nebulization, J. Anal. Atom. Spectrom., 14, 1433–1438, doi:10.1039/A901949I, 1999.

Bigler, M., Röthlisberger, R., Lambert, F., Stocker, T. F., and Wagenbach, D.: Aerosol deposited in East Antarctica over the last glacial cycle: Detailed apportionment of continental and sea-salt contributions, J. Geophys. Res., 111, D08205, doi:08210.01029/02005JD006469, 2006.

Bory, A., Wolff, E., Mulvaney, R., Jagoutz, E., Wegner, A., Ruth, U., and Elderfield, H.: Multiple sources supply eolian mineral dust to the Atlantic sector of coastal Antarctica: Evidence from recent snow layers at the top of Berkner Island ice sheet, Earth Planet. Sc. Lett., 291, 138–148, doi:10.1016/j.epsl.2010.01.006, 2010.

Buiron, D., Chappellaz, J., Stenni, B., Frezzotti, M., Baumgartner, M., Capron, E., Landais, A., Lemieux-Dudon, B., Masson-Delmotte, V., Montagnat, M., Parrenin, F., and Schilt, A.: TALDICE-1 age scale of the Talos Dome deep ice core, East Antarctica, Clim. Past, 7, 1–16, doi:10.5194/cp-7-1-2011, 2011.

Buiron, D., Stenni, B., Chappellaz, J., Landais, A., Baumgartner, M., Bonazza, M., Capron, E., Frezzotti, M., Kageyama, M., Lemieux-Dudon, B., Masson-Delmotte, V., Parrenin, F., Schilt, A., Selmo, E., Severi, M., Swingedouw, D., and Udisti, R.: Regional imprints of millennial variability during the MIS 3 period around Antarctica, Quaternary Sci. Rev., 48, 99–112, doi:10.1016/j.quascirev.2012.05.023, 2012.

Delmonte, B., Petit, J. R., Andersen, K. K., Basile-Doelsch, I., Maggi, V., and Ya Lipenkov, V.: Dust size evidence for opposite regional atmospheric circulation changes over east Antarctica during the last climatic transition, Clim. Dynam., 23, 427–438, doi:10.1007/s00382-004-0450-9, 2004.

Delmonte, B., Baroni, C., Andersson, P. S., Schoberg, H., Hansson, M., Aciego, S., Petit, J. R., Albani, S., Mazzola, C., Maggi, V., and Frezzotti, M.: Aeolian dust in the Talos Dome ice core (East Antarctica, Pacific/Ross Sea sector): Victoria Land versus remote sources over the last two climate cycles, J. Quat. Sci., 25, 1327–1337, doi:10.1002/jqs.1418, 2010.

Delmonte, B., Baroni, C., Andersson, P. S., Narcisi, B., Salvatore, M. C., Petit, J. R., Scarchilli, C., Frezzotti, M., Albani, S., and Maggi, V.: Modern and Holocene aeolian dust variability from Talos Dome (Northern Victoria Land) to the interior of the Antarctic ice sheet, Quaternary Sci. Rev., 64, 76–89, doi:10.1016/j.quascirev.2012.11.033, 2013.

Edwards, R., Sedwick, P. N., Morgan, V., and Boutron, C.: Iron in ice cores from Law Dome: A record of atmospheric iron deposition for maritime East Antarctica during the Holocene and Last Glacial Maximum, Geochem. Geophy. Geosys., 7, Q12Q01, doi:10.1029/2006GC001307, 2006.

Fischer, H., Siggaard-Andersen, M.-L., Ruth, U., Röthlisberger, R., and Wolff, E.: Glacial/interglacial changes in mineral dust and sea-salt records in polar ice cores: Sources, transport, and deposition, Rev. Geophys., 45, RG1002, doi:1010.1029/2005RG000192, doi, 2007.

Fischer, H., Schmitt, J., Luthi, D., Stocker, T. F., Tschumi, T., Parekh, P., Joos, F., Kohler, P., Volker, C., Gersonde, R., Barbante, C., Le Floch, M., Raynaud, D., and Wolff, E.: The role of Southern Ocean processes in orbital and millennial CO_2 variations – A synthesis, Quaternary Sci. Rev., 29, 193–205, doi:10.1016/j.quascirev.2009.06.007, 2010.

Gabrielli, P., Wegner, A., Petit, J. R., Delmonte, B., De Deckker, P., Gaspari, V., Fischer, H., Ruth, U., Kriews, M., Boutron, C. F., Cescon, P., and Barbante, C.: A major glacial-interglacial change in aeolian dust composition inferred from Rare Earth Elements in Antarctic ice, Quaternary Sci. Rev., 29, 265–273, doi:10.1016/j.quascirev.2009.09.002, 2010.

Gaspari, V., Barbante, C., Cozzi, G., Cescon, P., Boutron, C. F., Gabrielli, P., Capodaglio, G., Ferrari, C., Petit, J. R., and Delmonte, B.: Atmospheric iron fluxes over the last deglaciation: Climatic implications, Geophys. Res. Lett., 33, L03704, doi:10.1029/2005GL024352, 2006.

Kaufmann, P., Federer, U., Hutterli, M. A., Bigler, M., Schüpbach, S., Ruth, U., Schmitt, J., and Stocker, T. F.: An improved continuous flow analysis system for high-resolution field measurements on ice cores, Environ. Sci. Technol., 42, 8044–8050, doi:10.1021/es8007722, 2008.

Lambert, F., Delmonte, B., Petit, J. R., Bigler, M., Kaufmann, P. R., Hutterli, M. A., Stocker, T. F., Ruth, U., Steffensen, J. P., and Maggi, V.: Dust-climate couplings over the past 800,000 years from the EPICA Dome C ice core, Nature, 452, 616–619, doi:10.1038/nature06763, 2008.

Li, F., Ginoux, P., and Ramaswamy, V.: Distribution, transport, and deposition of mineral dust in the Southern Ocean and Antarctica: Contribution of major sources, J. Geophys. Res., 113, D10207, doi:10.1029/2007JD009190, 2008.

Lüthi, D., Floch, M. L., Bereiter, B., Blunier, T., Barnola, J.-M., Siegenthaler, U., Raynaud, D., Jouzel, J., Fischer, H., Kawamura, K., and Stocker, T. F.: High-resolution carbon dioxide concentration record 650,000–800,000 years before present, Nature, 453, 379–382, doi:10.1038/nature06949, 2008.

Maher, B., Prospero, J., Mackie, D., Gaiero, D. M., Hesse, P. P., and Balkanski, Y.: Global connections between aeolian dust, climate and ocean biogeochemistry at the present day and at the last glacial maximum, Earth-Sci. Rev., 99, 61–97, doi:10.1016/j.earscirev.2009.12.001, 2010.

Mahowald, N., Baker, A. R., Bergametti, G., Brooks, N., Duce, R. A., Jickells, T. D., Kubilay, N., Prospero, J. M., and Tegen, I.: Atmospheric global dust cycle and iron inputs to the ocean, Global Biogeochem. Cy., 19, GB4025, doi:10.1029/2004GB002402, 2005.

Martin, J. H., Gordon, R. M., and Fitzwater, S. E.: Iron in Antarctic waters, Nature, 345, 156–158, doi:10.1038/345156a0, 1990.

Martinez-Garcia, A., Rosell-Melé, A., Geibert, W., Gersonde, R., Masqué, P., Gaspari, V., and Barbante, C.: Links between iron supply, marine productivity, sea surface temperature, and CO_2 over the last 1.1 Ma, Paleoceanography, 24, PA1207, doi:10.1029/2008PA001657, 2009.

Röthlisberger, R., Mulvaney, R., Wolff, E. W., Hutterli, M. A., Bigler, M., Sommer, S., and Jouzel, J.: Dust and sea salt variability in central East Antarctica (Dome C) over the last 45 kyrs and its implications for southern high-Iatitude climate, Geophys. Res. Lett., 29, 1963, doi:10.1029/2002GL015186, 2002.

Röthlisberger, R., Bigler, M., Wolff, E. W., Joos, F., Monnin, E., and Hutterli, M. A.: Ice core evidence for the extent of past atmospheric CO_2 change due to iron fertilisation, Geophys. Res. Lett., 31, L16207, doi:10.1029/2004GL020338, 2004.

Schilt, A., Baumgartner, M., Schwander, J., Buiron, D., Capron, E., Chappellaz, J., Loulergue, L., Schüpbach, S., Spahni, R., Fischer, H., and Stocker, T. F.: Atmospheric nitrous oxide during the last 140,000 years, Earth Planet. Sc. Lett., 300, 33–43, doi:10.1016/j.epsl.2010.09.027, 2010.

Schüpbach, S., Federer, U., Bigler, M., Fischer, H., and Stocker, T. F.: A refined TALDICE-1a age scale from 55 to 112 ka before present for the Talos Dome ice core based on high-resolution methane measurements, Clim. Past, 7, 1001–1009, doi:10.5194/cp-7-1001-2011, 2011.

Sigman, D. M., Hain, M. P., and Haug, G. H.: The polar ocean and glacial cycles in atmospheric CO_2 concentration, Nature, 466, 47–55, doi:10.1038/nature09149, 2010.

Smetacek, V., Klaas, C., Strass, V. H., Assmy, P., Montresor, M., Cisewski, B., Savoye, N., Webb, A., d'Ovidio, F., Arrieta, J. M., Bathmann, U., Bellerby, R., Berg, G. M., Croot, P., Gonzalez, S., Henjes, J., Herndl, G. J., Hoffmann, L. J., Leach, H., Losch, M., Mills, M. M., Neill, C., Peeken, I., Rottgers, R., Sachs, O., Sauter, E., Schmidt, M. M., Schwarz, J., Terbruggen, A., and Wolf-Gladrow, D.: Deep carbon export from a Southern Ocean iron-fertilized diatom bloom, Nature, 487, 313–319, doi:10.1038/nature11229, 2012.

Spolaor, A., Vallelonga, P., Gabrieli, J., Cozzi, G., Boutron, C., and Barbante, C.: Determination of Fe^{2+} and Fe^{3+} species by FIA-CRC-ICP-MS in Antarctic ice samples, J. Ana. Atom. Spectrom., 27, 310–317, doi:10.1039/C1JA10276A, 2012.

Spolaor, A., Vallelonga, P., Cozzi, G., Gabrieli, J., Varin, C., Kehrwald, N., Zennaro, P., Boutron, C., and Barbante, C.: Iron speciation in aerosol dust influences iron bioavailability over glacial-interglacial timescales, Geophys. Res. Lett., online first, doi:10.1002/grl.50296, 2013.

Stenni, B., Buiron, D., Frezzotti, M., Albani, S., Barbante, C., Bard, E., Barnola, J. M., Baroni, M., Baumgartner, M., Bonazza, M., Capron, E., Castellano, E., Chappellaz, J., Delmonte, B., Falourd, S., Genoni, L., Iacumin, P., Jouzel, J., Kipfstuhl, S., Landais, A., Lemieux-Dudon, B., Maggi, V., Masson-Delmotte, V., Mazzola, C., Minster, B., Montagnat, M., Mulvaney, R., Narcisi, B., Oerter, H., Parrenin, F., Petit, J. R., Ritz, C., Scarchilli, C., Schilt, A., Schupbach, S., Schwander, J., Selmo, E., Severi, M., Stocker, T. F., and Udisti, R.: Expression of the bipolar see-saw in Antarctic climate records during the last deglaciation, Nat. Geosci., 4, 46–49, doi:10.1038/ngeo1026, 2011.

Vallelonga, P., Gabrielli, P., Balliana, E., Wegner, A., Delmonte, B., Turetta, C., Burton, G., Vanhaecke, F., Rosman, K. J. R., Hong, S., Boutron, C. F., Cescon, P., and Barbante, C.: Lead isotopic compositions in the EPICA Dome C ice core and Southern Hemisphere Potential Source Areas, Quaternary Sci. Rev., 29, 247–255, doi:10.1016/j.quascirev.2009.06.019, 2010.

Wegner, A., Gabrielli, P., Wilhelms-Dick, D., Ruth, U., Kriews, M., De Deckker, P., Barbante, C., Cozzi, G., Delmonte, B., and Fischer, H.: Change in dust variability in the Atlantic sector of Antarctica at the end of the last deglaciation, Clim. Past, 8, 135–147, doi:10.5194/cp-8-135-2012, 2012.

Wolff, E. W., Fischer, H., Fundel, F., Ruth, U., Twarloh, B., Littot, G. C., Mulvaney, R., Röthlisberger, R., de Angelis, M., Boutron, C. F., Hansson, M., Jonsell, U., Hutterli, M. A., Lambert, F., Kaufmann, P., Stauffer, B., Stocker, T. F., Steffensen, J. P., Bigler, M., Siggaard-Andersen, M. L., Udisti, R., Becagli, S., Castellano, E., Severi, M., Wagenbach, D., Barbante, C., Gabrielli, P., and Gaspari, V.: Southern Ocean sea-ice extent, productivity and iron flux over the past eight glacial cycles, Nature, 440, 491–496, doi:10.1038/nature04614, 2006.